Journal of Information Processing Vol.26 74–84 (Feb. 2018)

[DOI: 10.2197/ipsjjip.26.74]

Regular Paper

Development of a Visualization Method for Motion-characteristic Distribution of Japanese Folk Dances – A Case Study of the Bon Odori Dance

Takeshi Miura[1,a)] Takaaki Kaiga[2] Takeshi Shibata[3]
Madoka Uemura[4] Katsubumi Tajima[1] Hideo Tamamoto[5]

Received: May 1, 2017, Accepted: November 7, 2017

Abstract: This study proposes a method to systematically visualize the motion-characteristic distribution of Japanese folk dances passed down in a certain area. This is accomplished by adopting an approach that involves analyzing motion-capture data collected from the dances. The visualization process in the proposed method consists of three stages. The first stage is the modeling of the relationship among motion-capture data, folk dances, and the settlements in which folk dances have been passed down. This relationship is modeled as a hierarchical-structure model. The second stage is the extraction of motion characteristics from motion-capture data streams. The motion characteristics of each data stream are summarized as a fourteen-dimensional feature vector. The third stage is the visualization of the motion-characteristic distribution of the dances investigated. Each of the dances is mapped on a two-dimensional scatter plot in accordance with the feature quantities obtained in the second stage. Information on the hierarchical-structure model constructed in the first stage is also displayed. The analysis results for the distribution of Bon Odori dances showed that the proposed method could have almost completely visualized the motion-characteristic distribution of sample folk dances, while also demonstrating consistency with the knowledge of the dances acquired in the previous studies.

Keywords: Japanese folk dance, motion characteristic, motion capture, visualization

1. Introduction

Folk dances are one of the important constituents of Japanese folk performing arts, along with dramatic, narrative, and musical presentations [1]. Most Japanese folk dances have been performed in local events held in respective regional communities [1], [2]. Each of the folk dances has been strongly affected by the natural and cultural conditions of each region [3]. By investigating the variation in regional dancing-style and analyzing its relevance to the lifestyle of corresponding regions, traces of a lost traditional culture in a respective community may be found, or at least a slight clue may be provided.

According to Ref. [3], research activities on folk dances are grouped into three categories: motion analysis, study of music, and ethnological approach. In this study, we focus on motion analysis. The motion characteristics of Japanese folk dances have been investigated mainly from the qualitative viewpoint, as will be mentioned in "2. Related Work." Today, however, human-body motions can be accurately measured by using a motion-capture (Mocap) system [4]. Analyzing Mocap data allows us to evaluate the motion characteristics of folk dances in a more objective and quantitative manner. In particular, visualizing the quantitative motion-characteristic distribution of a large number of dances may provide us with clues to intuitively understand the relationship among the dances on a quantitative basis. However, there are very few studies that present a systematic approach to visualize the motion-characteristic distribution of folk dances.

Taking the above fact into consideration, we develop a new method to systematically visualize the distribution of the motion characteristics of Japanese folk dances passed down in a certain area by using Mocap data. The visualization process in the proposed method consists of three stages, which are described as follows.

The first stage is the modeling of the relationship among Mocap data, folk dances, and settlements in which respective regional communities have been formed. Here, the settlements in which a dance (or multiple dances) has been passed down are treated as objects for investigation, and it is assumed that a time-series Mocap data stream (or multiple data streams) was already acquired for each dance. In many previous studies, settlements in which folk dances have been passed down were grouped based on the similarity of dancing styles or that of manners and customs (examples will be shown in "3.1 Modeling of relationship

[1] Graduate School of Engineering Science, Akita University, Akita 010–8502, Japan
[2] Digital Art Factory, Warabi-za Co., Ltd., Semboku, Akita 014–1192, Japan
[3] Collage of Information and Systems, Muroran Institute of Technology, Muroran, Hokkaido 050–8585, Japan
[4] Faculty of Education and Human Studies, Akita University, Akita 010–8502, Japan
[5] Tohoku University of Community Service and Science, Sakata, Yamagata 998–8580, Japan
[a)] miura@mail.ee.akita-u.ac.jp

© 2018 Information Processing Society of Japan

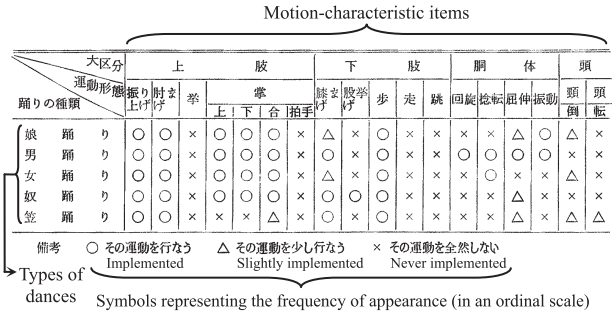

(a) Motion characteristics of folk dances passed down in the Kibi district (Table 2 in Ref. [8] is reproduced, English explanations: added by the authors).

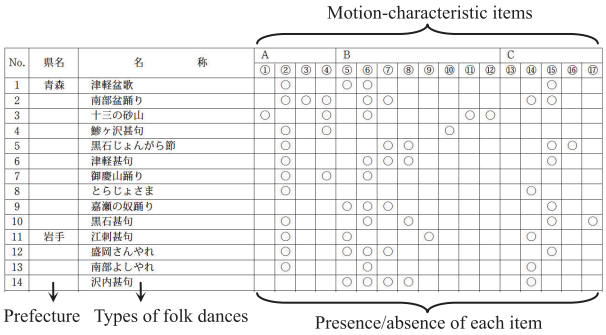

(b) Motion characteristics of folk dances passed down in the prefectures of Japan (Part of Material 2 in Ref. [10] is reproduced, English explanations: added by the authors).

Fig. 1 Examples of tables representing the qualitative categorization of motions in folk dances (reproduced from Refs. [8] and [10]).

among motion-capture data, folk dances and settlements"). We use the above grouping information in the modeling process. Finally, we construct a model representing the relationship among Mocap data, folk dances, and settlements, thereby introducing the concept of a hierarchical-structure model.

The second stage is the extraction of motion characteristics from Mocap data streams of the dances investigated. In this stage, we separately extract the time-domain feature quantities and the spatial-domain ones to systematically grasp the motion characteristics of each dance. To enable the comparison among many dances that may provide a wide range of different dancing styles, we adopt the analysis approaches proposed in Refs. [5] and [6]. These approaches provide the feature quantities of motion characteristics in a unified format, regardless of the difference in dancing styles. As a result, we obtain the information on the motion characteristics of each dance in the form of a feature vector with specified dimensionality (specifically, a fourteen-dimensional feature vector is obtained and will be shown later in "3.3 Extraction of spatial-domain motion characteristics").

The third stage is the visualization of the motion-characteristic distribution of the dances investigated. In this stage, each dance is mapped on a two-dimensional scatter plot in accordance with the feature quantities obtained in the second stage. Because the dimensionality of the feature vector obtained is larger than two, we develop a new dimensionality-reduction technique suitable for visualizing the motion-characteristic distribution of folk dances. Meanwhile, we define several graphic symbols to indicate the relationship among the dances and the settlements modeled in the first stage. The symbols are displayed on the scatter plot with the mapped dance points. To evaluate the proposed method, we conduct an analysis in which the Mocap data of actual Japanese folk dances are used. Specifically, a case study of the *Bon Odori* [*1] dances of the Akita Prefecture is shown.

2. Related Work

As previously mentioned in "1. Introduction," research activities on Japanese folk dances are categorized into motion analysis, study of music, and ethnological approach. As for the motion analysis that is the main subject of this study, many researchers have conducted studies to clarify the motion characteristics of Japanese folk dances passed down in their respective regional communities. The following studies represent typical examples of conventional approaches in which Mocap data were not used. Averbuch [7] examined three case studies of Japanese shamanic dances and discussed the preservation of shamanic choreography. Mimuro [3], [8], [9] investigated the folk dances passed down in the Kibi District (currently, Okayama Prefecture), and finally clarified the state of the geographical distribution of the dances to a certain extent. Yamada [10] tried to find the gestures in Japanese *Bon Odori* dances seen commonly throughout the country. As a result, several step patterns and hand gestures were extracted. In the above examples, the motion characteristics of dances were qualitatively examined. In the latter two examples, motions in each dance were qualitatively categorized and summarized in the form of a table (or a set of tables). Examples are shown in **Fig. 1**. As shown in the figure, presenting information on motion characteristics in the form of a table is useful for qualitatively comparing the characteristics of multiple dances in detail. However, it is difficult to intuitively and quantitatively grasp an overall view of their distribution. Schematically visualizing the motion-characteristic distribution has an advantage over table presentation in quantitatively examining an overall trend.

There have been several examples where Mocap techniques have been applied in the motion analysis of folk dances. Usui et al. [11] attempted to use the Mocap data of Japanese folk dances (specifically, *Minbu* [*2] and *Kagura* [*3]) for dance practice. They found that students could have gained an objective perspective by deliberately reducing the information in computer animations of the Mocap data. Kitsikidis et al. [12] proposed a method for the partitioning of dance sequences into motion patterns. In their method, the Hidden Markov Models (HMMs) [13] technique was used to identify each motion pattern. They applied their method to the practice of the Greek *Tsamiko* dance and confirmed its effectiveness. Aristidou et al. [14] proposed a framework for teaching Cypriot folk dances. In their study, the Mocap data collected

[*1] *Bon Odori* is a type of Japanese folk dance performed during the annual Buddhist festival called *O-Bon* (or simply *Bon*) [1].

[*2] *Minbu* is a type of Japanese folk dance created in accordance with the folk music passed down in each region [11].

[*3] *Kagura* is a type of Japanese folk dance performed as a ritual to pray for good harvest, good fish and good health [11].

© 2018 Information Processing Society of Japan

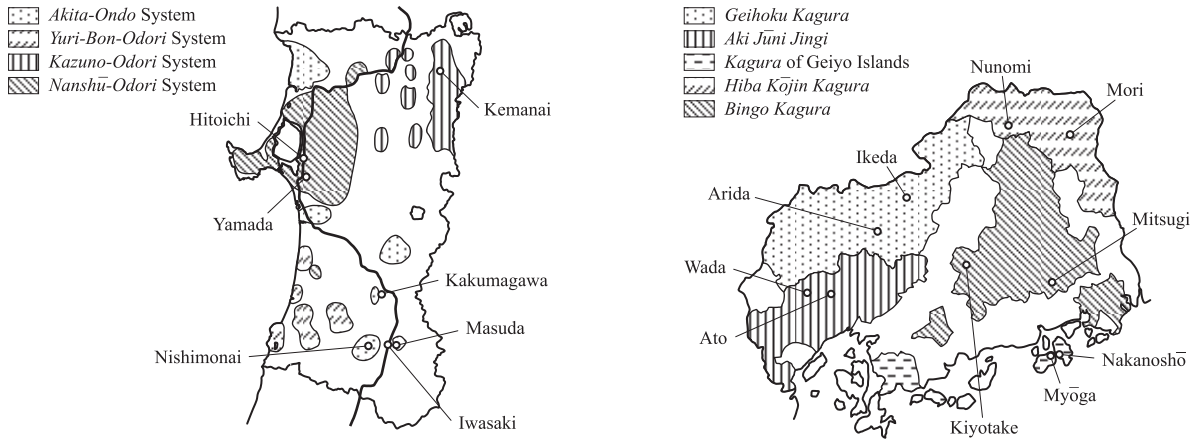

(a) *Bon Odori* of Akita Prefecture.

(b) *Kagura* of Hiroshima Prefecture.

Fig. 2 Examples of distribution maps of Japanese folk dances. (a): created by tracing the map on page 17 of Ref. [16], (b): created on the basis of the data of Tables 9, 1-1, 2-1, 3-1, 4-1, 5-1 in Ref. [17], ∘ : settlement where a folk dance (or a set of folk dances) has been passed down.

from students were compared with those of their teachers based on the Laban Movement Analysis (LMA) [15].

Part of the above examples [12], [14] provided methods to compare the motion characteristics of multiple Mocap data streams. In the methods, an entire dance sequence is first partitioned into short-duration motion patterns, and feature quantities are then extracted at every motion pattern. Finally, the extracted motion characteristics are compared at every pair of motion patterns extracted from each of the data streams compared. Although this approach enables the detailed comparison of the individual constituents comprising each data stream, the overall tendency of an entire sequence of each data stream is not taken into account.

To visualize the distribution of many dances by mapping them on a scatter plot, using a feature quantity (or feature quantities) that represents the overall motion-characteristic tendency of each dance is preferable than using the information on too finely partitioned motion patterns. Therefore, we do not use the above approach, but adopt the approaches proposed in Refs. [5] and [6] as mentioned in "1. Introduction." These approaches evaluate the overall tendency of an entire dance sequence, regardless of the difference in motion styles, such as the number of motion patterns, and the length of a dance sequence.

3. Visualization of Motion-characteristic Distribution

3.1 Modeling of Relationship among Motion-capture Data, Folk Dances, and Settlements

In this section, we present the visualization process of the motion-characteristic distribution of folk dances. We first construct a model that represents the relationship among Mocap data, folk dances, and the settlements in which folk dances have been passed down. This is the first stage of the visualization process. As mentioned in "1. Introduction," we use the information on the grouping of settlements, which are representative places where folk dances have been passed down, based on the similarity of dancing styles or that of manners and customs. **Figure 2** shows examples of this type of grouping. Example (a) shows the grouping of *Bon Odori* dances in the Akita Prefecture [16], whereas (b) shows that of *Kagura* dances in the Hiroshima Prefecture [17]. In both cases, particular areas (e.g., area belonging to the *Akita-Ondo* [*4] System in Example (a), etc.) were grouped based on the similarity of the characteristics of the dances passed down. In each of the grouped areas, there is a settlement (or multiple settlements) where a folk dance (or multiple folk dances) has been passed down (e.g., Iwasaki in Example (a), etc.). As previously mentioned in "1. Introduction," it is assumed that a Mocap data stream (or multiple data streams) was already acquired for each dance.

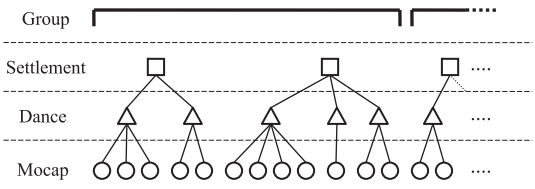

Constituents of each level

Group: a set of settlements where folk dances of the same type have been passed down.
(e.g., *Akita-Ondo* System, *Yuri-Bon-Odori* System, *Geihoku Kagura* and *Aki Jūni Jingi* in Fig. 2)

Settlement: a village or town where a folk dance (or a set of folk dances) has been passed down.
(e.g., Hitoichi, Yamada, Arida and Ikeda in Fig. 2)

Dance: a folk dance passed down in each settlement.

Mocap: a time-series Mocap data stream acquired in a folk-dance performance.

Fig. 3 Hierarchical-structure model of folk-dance distribution.

The above relationship can be modeled in a hierarchical structure, as shown in **Fig. 3**. The groups comprising the highest "Group" level correspond to the areas grouped in Fig. 2. Each of the groups includes a set of settlements, and each of the settlements provides a set of dances passed down in it. They comprise the second and third levels in the hierarchical structure (i.e., the "Settlement" and "Dance" levels). Furthermore, there are sets of Mocap data streams, each corresponding to any of the dances, in the lowest "Mocap" level. In this study, we aim at visualizing

[*4] *Akita Ondo* is a folk song passed down in part of Akita Prefecture, and used as the musical accompaniment of the dances belonging to the *Akita-Ondo* System [16].

© 2018 Information Processing Society of Japan

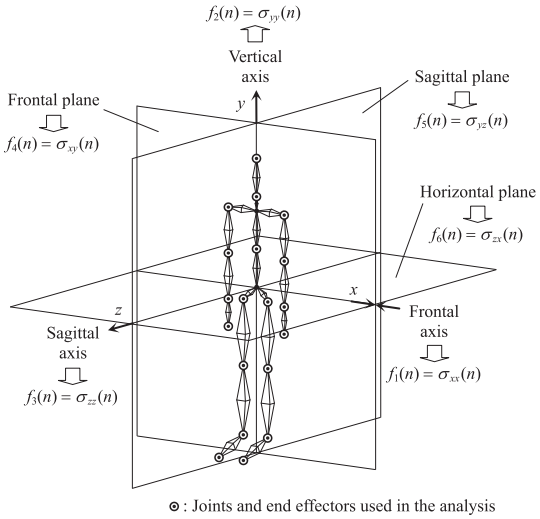

Fig. 4 Human-body model and the axes and planes of movement.

the motion-characteristic distribution of the dances by considering the above hierarchical structure.

3.2 Extraction of Time-domain Motion Characteristics

The next stage for visualizing the motion-characteristic distribution of folk dances is the extraction of feature quantities from Mocap data streams. The constituents of the "Mocap" level are characterized in this stage. As previously mentioned in "1. Introduction," we separately extract the quantities of time-domain motion characteristics and those of spatial-domain characteristics. In this section, we describe a method to extract the time-domain feature quantities. Here, we regard the time-domain characteristics as those that characterize the temporal variation of whole-body motion, without making a fine distinction among individual body segments. According to Ref. [3], the variation of motion speed is the most clearly perceptible factor in dance motion. Taking this opinion into consideration, we try to extract the feature quantities from the temporal variation of whole-body motion speed. We adopt the method proposed in Ref. [5] as shown below.

First, the whole-body motion-speed data stream is obtained from the temporal variation of the positions of the principal joints shown in **Fig. 4** (i.e., shoulders, elbows, wrists, fingers, hips, knees, ankles, toes, waist, neck and head, including end effectors) as follows:

$$v(n) = \frac{\sqrt{\sum_{j=1}^{J} \sum_{\gamma=x,y,z} \{p_{j,\gamma}(n+1) - p_{j,\gamma}(n)\}^2}}{\Delta t} \tag{1}$$

where $p_{j,\gamma}(n)$ (γ: x, y or z) is the γ-coordinate of the jth joint at the nth frame (coordinate system: fixed to the pelvis), J is the number of the principal joints taken into account ($J = 19$) and Δt is the sampling time. The values of $p_{j,\gamma}(n)$ are filtered to eliminate jitter (by using a Gaussian filter, cut-off frequency: 9.0 Hz), and normalized by the body height to reduce the influence of differences in physical constitution.

Next, two time-domain feature quantities characterizing the rhythmical aspect of dance motion are obtained from $v(n)$. The first quantity is the beat intensity and the second one is the rhythm complexity. The original formulation of the beat intensity (BI) shown in Ref. [5] is given as follows:

$$q_{\mathrm{BI}} = \frac{\sqrt{\sum_{n=1}^{N} \{v(n) - v_0(n)\}^2 / N}}{\tau \Delta t} \tag{2}$$

where τ is the frame number giving the first positive peak of the autocorrelation of $v(n)$, $v_0(n)$ is the moving average of $v(n)$ (moving average time: τ) and N is the total number of frames, respectively. Because the value, $\tau\Delta t$, gives the period of the periodic variation of $v(n)$, the denominator of Eq. (2) is regarded as the pace of tempo in dance motion. However, the numerator of Eq. (2) is the root mean square of motion-speed variation based on the moving average value, and gives the strength of motion-speed surges, inducing beats. As a result, the faster the tempo or the greater the motion-speed variation, the larger the value of q_{BI}.

However, it was pointed out in Ref. [5] that square-root values of q_{BI} gave more appropriate analysis results. This means that q_{BI} should be transformed into a new value by using a monotonously increasing function whose derivative monotonously decreases, such as a square root function. To resolve the above issue, we use a logarithm transform [18] as follows:

$$q_{\mathrm{BI}} = \frac{1}{2} \log \frac{\sum_{n=1}^{N} \{v(n) - v_0(n)\}^2}{N} - A \log(\tau \Delta t) \tag{3}$$

where A is the weighting coefficient to the element corresponding to the pace of the tempo, $\tau\Delta t$. A is newly introduced to enable adjusting the weighting ratio between the motion-speed-surge element (i.e., the first term of Eq. (3)) and the pace-of-tempo element (i.e., the second term of Eq. (3)). We set $A = 0.2$ according to Ref. [18].

As for the rhythm complexity, we use the value of approximate entropy (ApEn) [19]. ApEn is known as an index that represents the complexity of a time-series data stream. The value of ApEn is calculated as follows:

$$\begin{aligned}
&\boldsymbol{\mu}(n) = [v(n) \;\; v(n+\tau') \;\; \cdots \;\; v(n+(m-1)\tau')]^{\mathrm{T}} \\
&d(\boldsymbol{\mu}(n), \boldsymbol{\mu}(j)) = \max_{k=1,2,\cdots,m} (|v(n+(k-1)\tau') - v(j+(k-1)\tau')|) \\
&C_n^m = \frac{\sum_{j=1}^{N-(m-1)\tau'} \theta(r - d(\boldsymbol{\mu}(n), \boldsymbol{\mu}(j)))}{N-(m-1)\tau'} \\
&\Phi^m = \frac{\sum_{n=1}^{N-(m-1)\tau'} \log C_n^m}{N-(m-1)\tau'} \\
&q_{\mathrm{ApEn}} = \Phi^m - \Phi^{m+1}
\end{aligned} \tag{4}$$

where $\tau' = \mathrm{round}(0.2\tau)$, $m = 4$, $r = 0.5 \times$ (standard deviation of $v(n)$) and $\theta(x)$ is the Heaviside function. Equation (4) includes the time-delay parameter [20], τ', that is not included in the original ApEn [19]. We introduce τ' because the time scale of human motion is generally much longer than the sampling time of Mocap data Δt. The value of q_{ApEn} becomes large when $v(n)$ shows a complex and irregular waveform. In actual calculations, we use a fast algorithm [21] to reduce the calculation time. In summary, the time-domain motion characteristics are represented as the following two-dimensional feature vector, $\boldsymbol{F}_{\mathrm{T}}$:

$$\boldsymbol{F}_{\mathrm{T}} = [\; q_{\mathrm{BI}} \quad q_{\mathrm{ApEn}} \;]^{\mathrm{T}} \tag{5}$$

3.3 Extraction of Spatial-domain Motion Characteristics

In this section, we describe a method to extract the spatial-domain feature quantities. As mentioned in "1. Introduction," we

© 2018 Information Processing Society of Japan

adopt the method proposed in Ref. [6] as follows. First, we extract quantities representing the spatial arrangement of the body segments at each instant of time. Specifically, we use the variances and covariances of the coordinates of the joints shown in Fig. 4 as follows:

$$\bar{p}_\gamma(n) = \frac{1}{J}\sum_{j=1}^{J} p_{j,\gamma}(n) \qquad (\gamma : x, y \text{ or } z)$$

$$\sigma_{\gamma\eta}(n) = \frac{1}{J}\sum_{j=1}^{J}\{p_{j,\gamma}(n) - \bar{p}_\gamma(n)\}\{p_{j,\eta}(n) - \bar{p}_\eta(n)\} \tag{6}$$

$\sigma_{xx}(n)$, $\sigma_{yy}(n)$ and $\sigma_{zz}(n)$ give the spread of the body segments along the three axes of movement (i.e., the frontal, vertical and sagittal axes [22]), whereas $\sigma_{xy}(n)$, $\sigma_{yz}(n)$ and $\sigma_{zx}(n)$ provide the spread of the body segments on the three planes of movement (i.e., the frontal, sagittal and horizontal planes [22]). We regard these values as the components of the feature vector, $\boldsymbol{f}(n)$, that characterize a posture in the nth frame as follows:

$$\begin{aligned}\boldsymbol{f}(n) &= [\ f_1(n)\quad f_2(n)\quad f_3(n)\quad f_4(n)\quad f_5(n)\quad f_6(n)\ ]^{\mathrm{T}}\\ &= [\ \sigma_{xx}(n)\quad \sigma_{yy}(n)\quad \sigma_{zz}(n)\quad \sigma_{xy}(n)\quad \sigma_{yz}(n)\quad \sigma_{zx}(n)\ ]^{\mathrm{T}}\end{aligned} \tag{7}$$

Each component corresponds to the spread in each of the axes or planes of movement as shown in Fig. 4.

Next, the trend throughout an entire Mocap data stream is statistically summarized as the twelve-dimensional feature vector, $\boldsymbol{F}_{\mathrm{S}}$, as follows:

$$\bar{f}_i = \frac{1}{N}\sum_{n=1}^{N} f_i(n) \qquad (= \sigma_{\gamma\eta\,\mathrm{mean}})$$

$$\bar{s}_i = \sqrt{\frac{1}{N}\sum_{n=1}^{N}\{f_i(n) - \bar{f}_i\}^2} \qquad (= \sigma_{\gamma\eta\,\mathrm{SD}})$$

$$\begin{aligned}\boldsymbol{F}_{\mathrm{S}} &= [\ \bar{f}_1\quad \bar{f}_2\quad \cdots\quad \bar{f}_6\quad \bar{s}_1\quad \bar{s}_2\quad \cdots\quad \bar{s}_6]^{\mathrm{T}}\\ &= [\ \sigma_{xx\,\mathrm{mean}}\quad \cdots\quad \sigma_{zx\,\mathrm{mean}}\quad \sigma_{xx\,\mathrm{SD}}\quad \cdots\quad \sigma_{zx\,\mathrm{SD}}]^{\mathrm{T}}\end{aligned} \tag{8}$$

where the $\bar{f}_i$'s represent the average amounts of spread throughout an entire data stream (former three: spread along the three axes of movement, latter three: spread on the three planes of movement), whereas the $\bar{s}_i$'s represent the fluctuations of spread during an entire data stream (also corresponding to the axes and planes of movement). We use these twelve values as the spatial-domain feature quantities.

As a result, the motion characteristics of each Mocap data stream, including both the time- and spatial-domain characteristics, are represented as the following fourteen-dimensional feature vector $\boldsymbol{Q}$:

$$\begin{aligned}\boldsymbol{Q} &= [\ \boldsymbol{F}_{\mathrm{T}}^{\mathrm{T}}\quad \boldsymbol{F}_{\mathrm{S}}^{\mathrm{T}}\ ]^{\mathrm{T}}\\ &= [\ q_{\mathrm{BI}}\quad q_{\mathrm{ApEn}}\quad \bar{f}_1\quad \bar{f}_2\quad \cdots\quad \bar{f}_6\quad \bar{s}_1\quad \bar{s}_2\quad \cdots\quad \bar{s}_6]^{\mathrm{T}}\\ &= [\ q_{\mathrm{BI}}\quad q_{\mathrm{ApEn}}\\ &\qquad \sigma_{xx\,\mathrm{mean}}\quad \cdots\quad \sigma_{zx\,\mathrm{mean}}\quad \sigma_{xx\,\mathrm{SD}}\quad \cdots\quad \sigma_{zx\,\mathrm{SD}}]^{\mathrm{T}}\end{aligned} \tag{9}$$

3.4 Dimensionality Reduction

As shown in Eq. (9), the motion characteristics of a given Mocap data stream are represented as a fourteen-dimensional feature vector. To visualize the motion-characteristic distribution on a two-dimensional scatter plot, we must reduce the dimensionality in an appropriate manner. In this section, we present a dimensionality-reduction technique suitable for visualizing the motion-characteristic distribution of folk dances. This is the third stage of visualization.

In the visualization process, we take the following two items (hereinafter, Items (1) and (2)) into account:

(1) Assigning the same weight to both the set of the time-domain feature quantities, $\boldsymbol{F}_{\mathrm{T}}$, and that of the spatial-domain feature quantities, $\boldsymbol{F}_{\mathrm{S}}$. We introduce this item to avoid underestimating the influence of the time-domain quantities consisting of only two of the fourteen quantities.

(2) Assigning the same weight to each set of the Mocap data streams corresponding to the same dance, i.e., assigning the same weight to each of the dances investigated. We introduce this item to eliminate the influence of the difference in the Mocap-data-stream numbers of respective dances.

To satisfy the requirements of the above items, we adopt the approach proposed in Ref. [23] as shown below.

First, each of the fourteen quantities is standardized (with zero mean and unity standard deviation) throughout all the Mocap data streams used in the analysis. After the standardization, the normalized distance (with unity mean) of each of all the Mocap-data-stream pairs in the $\boldsymbol{F}_{\mathrm{T}}$ space (two dimensional), and that in the $\boldsymbol{F}_{\mathrm{S}}$ space (twelve dimensional), are calculated as follows:

$$d'_{\mathrm{T}}(j,k) = \sqrt{\{q'_{\mathrm{BI}}(j) - q'_{\mathrm{BI}}(k)\}^2 + \{q'_{\mathrm{ApEn}}(j) - q'_{\mathrm{ApEn}}(k)\}^2}$$

$$d'_{\mathrm{S}}(j,k) = \sqrt{\sum_{i=1}^{6}[\{\bar{f}'_i(j) - \bar{f}'_i(k)\}^2 + \{\bar{s}'_i(j) - \bar{s}'_i(k)\}^2]}$$

$$\bar{d}_{\mathrm{T}} = \frac{1}{M^2}\sum_{j=1}^{M}\sum_{k=1}^{M} d'_{\mathrm{T}}(j,k)$$

$$\bar{d}_{\mathrm{S}} = \frac{1}{M^2}\sum_{j=1}^{M}\sum_{k=1}^{M} d'_{\mathrm{S}}(j,k)$$

$$d_{\mathrm{T}}(j,k) = d'_{\mathrm{T}}(j,k)/\bar{d}_{\mathrm{T}} \tag{10}$$

$$d_{\mathrm{S}}(j,k) = d'_{\mathrm{S}}(j,k)/\bar{d}_{\mathrm{S}} \tag{11}$$

where $q'_{\mathrm{BI}}(j)$ and $q'_{\mathrm{ApEn}}(j)$ are the standardized BI and ApEn of the jth Mocap data stream, $\bar{f}'_i(j)$ and $\bar{s}'_i(j)$ are the standardized spatial-domain feature quantities of the jth data stream, M is the total number of data streams, and $d_{\mathrm{T}}(j,k)$ and $d_{\mathrm{S}}(j,k)$ are the normalized distance between the jth and kth data streams in the $\boldsymbol{F}_{\mathrm{T}}$ space and that in the $\boldsymbol{F}_{\mathrm{S}}$ space, respectively.

Next, the normalized distance of each Mocap-data-stream pair, including both the time- and spatial-domain feature quantities, is calculated as follows:

$$D'(j,k) = \sqrt{d_{\mathrm{T}}(j,k)^2 + d_{\mathrm{S}}(j,k)^2}$$

$$\bar{D} = \frac{1}{M^2}\sum_{j=1}^{M}\sum_{k=1}^{M} D'(j,k)$$

$$D(j,k) = D'(j,k)/\bar{D} \tag{12}$$

where $D(j,k)$ is the normalized distance between the jth and kth Mocap data streams. In Eq. (12), the distance in the $\boldsymbol{F}_{\mathrm{T}}$ space and that in the $\boldsymbol{F}_{\mathrm{S}}$ space are evaluated with the same weighting. As a

© 2018 Information Processing Society of Japan

result, the requirement of Item (1) is satisfied.

Then, the distances of all dance pairs are calculated. To satisfy the requirement of Item (2) (assignment of the same weight to each dance), we use the Earth Mover's Distance (EMD) [24] as follows:

$$D_{\mathrm{EMD}}(\mathrm{P},\mathrm{Q}) = \frac{\sum_{j=1}^{M_\mathrm{P}} \sum_{k=1}^{M_\mathrm{Q}} D(j,k)u(j,k)}{\sum_{j=1}^{M_\mathrm{P}} \sum_{k=1}^{M_\mathrm{Q}} u(j,k)} \tag{13}$$

where $D_{\mathrm{EMD}}(\mathrm{P},\mathrm{Q})$ is the EMD between the P and Q dances, $u(j,k)$ is the "flow" from the jth Mocap data stream to the kth one (obtained by solving a transportation problem [24]), and M_P and M_Q are the number of the data streams included in the data set of the P dance and that of the Q dance, respectively. In Eq. (13), the jth Mocap data stream belongs to the P dance and the kth Mocap data stream belongs to the Q dance. Here, we solve the transportation problem under the following conditions:

$$\sum_{k=1}^{M_\mathrm{Q}} u(j,k) = \frac{1}{M_\mathrm{P}}, \quad \sum_{j=1}^{M_\mathrm{P}} u(j,k) = \frac{1}{M_\mathrm{Q}} \tag{14}$$

This means that every dance is evaluated with the same weighting, regardless of the difference in the Mocap-data-stream numbers of the respective dances. Consequently, the requirement of Item (2) is satisfied. However, in the calculation of EMD, the dispersion of a set of Mocap data streams belonging to the same dance is reflected in the value of distance. The condition of the dispersion of dancing style may imply a characteristic peculiar to each dance, and EMD provides information related to this condition. This can be regarded as an additional advantage of adopting EMD.

After calculating the EMDs of all dance pairs, every dance is mapped on a two-dimensional scatter plot by multidimensional scaling (MDS) [25]. Because the normalized distance $D(j,k)$ used in Eq. (13) is the Euclidean distance (i.e., metric), and the total weight of a set of Mocap data streams belonging to the same dance is unified by the conditions of Eq. (14), the EMD used in this study becomes a true metric [24]. Hence, we apply a technique of metric MDS [25] to the obtained set of EMDs. Therefore, the mapping of all the constituents of the "Dance" level is completed.

However, to map Mocap data streams that are the constituents of the "Mocap" level, we formulate the conversion from the fourteen-dimensional feature vector, $\boldsymbol{Q}$, to the components of a two-dimensional scatter plot $[\ q_1 \quad q_2\ ]^\mathrm{T}$. We use a multiple linear regression model [26] shown below:

$$\begin{aligned} q_i = {} & \beta_{i1} q'_{\mathrm{BI}} + \beta_{i2} q'_{\mathrm{ApEn}} + \beta_{i3} \bar{f}'_1 + \cdots + \beta_{i8} \bar{f}'_6 \\ & + \beta_{i9} \bar{s}'_1 + \cdots + \beta_{i14} \bar{s}'_6 + \beta_{i0}(\mathrm{P}) \end{aligned} \tag{15}$$

where q_i ($i = 1$ or 2) is the coordinate on the ith axis of a scatter plot, β_{ij}'s ($j = 1, 2, \cdots, 14$) are the partial regression coefficients and $\beta_{i0}(\mathrm{P})$ is the constant corresponding to the P dance (changed at every dance), respectively. On the right side of Eq. (15), the components of $\boldsymbol{Q}$ are used as predictor variables, whereas each of the components of $[\ q_1 \quad q_2\ ]^\mathrm{T}$ is used as a response variable on the left side. The values of β_{ij}'s are obtained by weighted linear regression analysis [26]. In the analysis, all the $\boldsymbol{Q}$'s of the Mocap data streams investigated are used as samples of the predictor variables, and each of the coordinate values of $[\ q_1 \quad q_2\ ]^\mathrm{T}$ of the dance corresponding to each sample Mocap data stream is used as a sample of the response variable. The weight for the jth sample Mocap data stream is given as follows:

$$w_j = \frac{1}{M_\mathrm{P}} \tag{16}$$

where M_P is the number of the Mocap data streams belonging to the P dance, which the jth Mocap data stream also belongs. This weight is set to give every dance the same total weight (this condition corresponds to Item (2)). The value of $\beta_{i0}(\mathrm{P})$ in Eq. (15) is given at every dance as follows:

$$\begin{aligned} \beta_{i0}(\mathrm{P}) = {} & q_i(\mathrm{P}) - \beta_{i1} q'_{\mathrm{BI}}|_\mathrm{P} - \beta_{i2} q'_{\mathrm{ApEn}}|_\mathrm{P} \\ & - \beta_{i3} \bar{f}'_1|_\mathrm{P} - \cdots - \beta_{i8} \bar{f}'_6|_\mathrm{P} - \beta_{i9} \bar{s}'_1|_\mathrm{P} - \cdots - \beta_{i14} \bar{s}'_6|_\mathrm{P} \end{aligned} \tag{17}$$

where $q_i(\mathrm{P})$ is the coordinate of the P dance on the ith axis of a scatter plot and $\zeta|_\mathrm{P}$ is the mean of the quantity, ζ, in the set of the Mocap data steams belonging to the dance P, respectively. Eq. (17) is introduced to fit the location of a dance to the centroid of the Mocap data streams belonging to this dance.

3.5 Graphic Symbols for the Visualization of the Relationship among Motion-capture Data, Folk Dances, and Settlements

The locations of the constituents of the "Dance" and "Mocap" levels in a two-dimensional scatter plot are determined by the procedures mentioned in Sections 3.2, 3.3 and 3.4. Here, we define a visualization format of the graphic symbols that indicates the relationship of the constituents of the "Group" and "Settlement" levels with those of the "Dance" and "Mocap" levels. Displaying the above information according to the defined format is the final procedure required to systematically visualize the motion-characteristic distribution of folk dances.

Figure 5 shows the visualization format. First, dances and Mocap data streams are plotted. The large circles in Fig. 5 are dances and the small circles are Mocap data streams. The first axis of the scatter plot (i.e., Axis 1 in Fig. 5) is set to give the largest standard deviation of the coordinate values of the dances in all axes.

Next, the information on the "Settlement" level is displayed. Dances belonging to the same settlement are connected by straight lines. The lines are arranged to form a minimum spanning tree [27]. The values of EMD are used as the edge lengths evaluated in the minimum-spanning-tree analysis. We adopted a minimum spanning tree in order to indicate the distribution of dances at each settlement as simply as possible, i.e., with a minimized number of lines kept as short as possible.

Then, the information on the "Group" level is displayed. Dances belonging to the same group are surrounded by a set of broken lines constituting a closed loop that represents the region of the group. The closed loop can be obtained by drawing a convex hull [27] enclosing all the dance points belonging to the same group. Specifically, a convex hull enclosing all the auxiliary points added to each of the dance points is used. The auxiliary points are added to intelligibly display the region of each group. Eight auxiliary points are plotted around each dance point as shown in Fig. 5 (these points are not displayed in an actual

© 2018 Information Processing Society of Japan

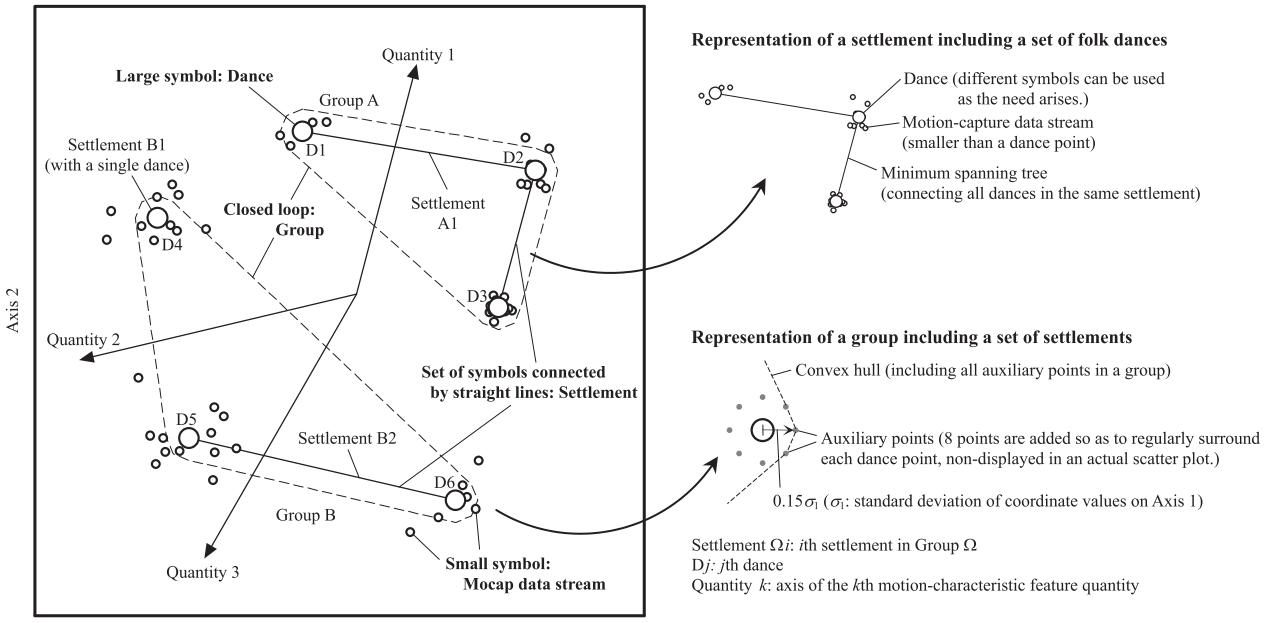

Fig. 5 Visualization format of motion-characteristic distribution.

scatter plot). The distance between a dance point and each of the auxiliary points is set to $0.15\sigma_1$ (σ_1: standard deviation of the coordinate values on Axis 1).

Finally, the axes of influential motion-characteristic feature quantities are drawn. As for a scatter plot obtained by MDS, the process of interpreting the meaning of each axis is often tedious, and sometimes requires extensive knowledge of analysis objects. Automatically displaying the axes representing influential characteristics allows us to easily grasp the meaning of the constellation obtained by MDS, without exerting the effort needed to interpret the meanings of the horizontal and vertical axes of the scatter plot itself. The arrowed lines in Fig. 5 are the axes of the feature quantities that are selected as influential characteristics. The axes of the feature quantities are obtained by using the correlation coefficients between the components of a scatter plot and the feature quantities as follows:

$$\boldsymbol{A}_{\mathrm{BI}} = R^{\mathrm{BI}}_{q_1,q_2} \frac{\begin{bmatrix} r^{q_2}_{\mathrm{BI},q_1} & r^{q_1}_{\mathrm{BI},q_2} \end{bmatrix}^{\mathrm{T}}}{\left| \begin{bmatrix} r^{q_2}_{\mathrm{BI},q_1} & r^{q_1}_{\mathrm{BI},q_2} \end{bmatrix}^{\mathrm{T}} \right|} \tag{18}$$

$$\boldsymbol{A}_{\mathrm{ApEn}} = R^{\mathrm{ApEn}}_{q_1,q_2} \frac{\begin{bmatrix} r^{q_2}_{\mathrm{ApEn},q_1} & r^{q_1}_{\mathrm{ApEn},q_2} \end{bmatrix}^{\mathrm{T}}}{\left| \begin{bmatrix} r^{q_2}_{\mathrm{ApEn},q_1} & r^{q_1}_{\mathrm{ApEn},q_2} \end{bmatrix}^{\mathrm{T}} \right|} \tag{19}$$

$$\boldsymbol{A}_{\bar{f}_i} = R^{\bar{f}_i}_{q_1,q_2} \frac{\begin{bmatrix} r^{q_2}_{\bar{f}_i,q_1} & r^{q_1}_{\bar{f}_i,q_2} \end{bmatrix}^{\mathrm{T}}}{\left| \begin{bmatrix} r^{q_2}_{\bar{f}_i,q_1} & r^{q_1}_{\bar{f}_i,q_2} \end{bmatrix}^{\mathrm{T}} \right|} \tag{20}$$

$$\boldsymbol{A}_{\bar{s}_i} = R^{\bar{s}_i}_{q_1,q_2} \frac{\begin{bmatrix} r^{q_2}_{\bar{s}_i,q_1} & r^{q_1}_{\bar{s}_i,q_2} \end{bmatrix}^{\mathrm{T}}}{\left| \begin{bmatrix} r^{q_2}_{\bar{s}_i,q_1} & r^{q_1}_{\bar{s}_i,q_2} \end{bmatrix}^{\mathrm{T}} \right|} \tag{21}$$

where $\boldsymbol{A}_\zeta$ is the vector representing the direction and magnitude of the axis of the feature quantity, ζ, $R^{\zeta}_{a,b}$ is the multiple correlation coefficient between ζ and a set of the variables a and b, and $r^{b}_{\zeta,a}$ is the partial correlation coefficient between ζ and a holding b fixed. In the calculation of Eqs. (18) to (21), all the Mocap data streams investigated are used as samples, and the weighted correlation coefficients [28] are used to satisfy the requirement of Item (2) in "3.4. Dimensionality reduction" (weight of each Mocap data stream: given by Eq. (16)). The axes that have a large magnitude, i.e., show a high correlation between the components of a scatter plot and a particular feature quantity, are regarded as those of influential motion-characteristic feature quantities.

4. Results and Discussion

4.1 Folk Dances Used as Sample Objects

This section presents an example application of the proposed method. The folk dances shown in Fig. 2 (a), i.e., the *Bon Odori* dances of the Akita Prefecture, are used as sample objects. As shown in this figure, *Bon Odori* dances of the Akita Prefecture are classified into four groups: *Akita-Ondo*, *Yuri-Bon-Odori*, *Kazuno-Odori* and *Nanshū-Odori* Systems. This grouping was proposed based on the condition of the dances in 1937 [16]. However, most of the dances belonging to the *Yuri-Bon-Odori* System have been lost until now [29]. Therefore, we analyze only the dances belonging to the three groups, i.e., the *Akita-Ondo*, *Kazuno-Odori* and *Nanshū-Odori* Systems. **Figure 6** shows the hierarchical-structure model of the analyzed folk dances. The dances passed down in the seven settlements shown in Fig. 2 (a) are analyzed. The forty Mocap data streams corresponding to the fourteen folk dances are used in the analysis.

4.2 Results

Figure 7 shows the scatter plot obtained by the proposed method. The items and scales of the vertical and horizontal axes were adjusted to make it easier to grasp the relationship to the map shown in Fig. 2 (a). The top four feature-quantity axes were displayed as representative influential motion-characteristic quantities.

It can be observed from the figure that the three groups formed their respective clusters, and the cluster of the *Akita-Ondo* Sys-

© 2018 Information Processing Society of Japan

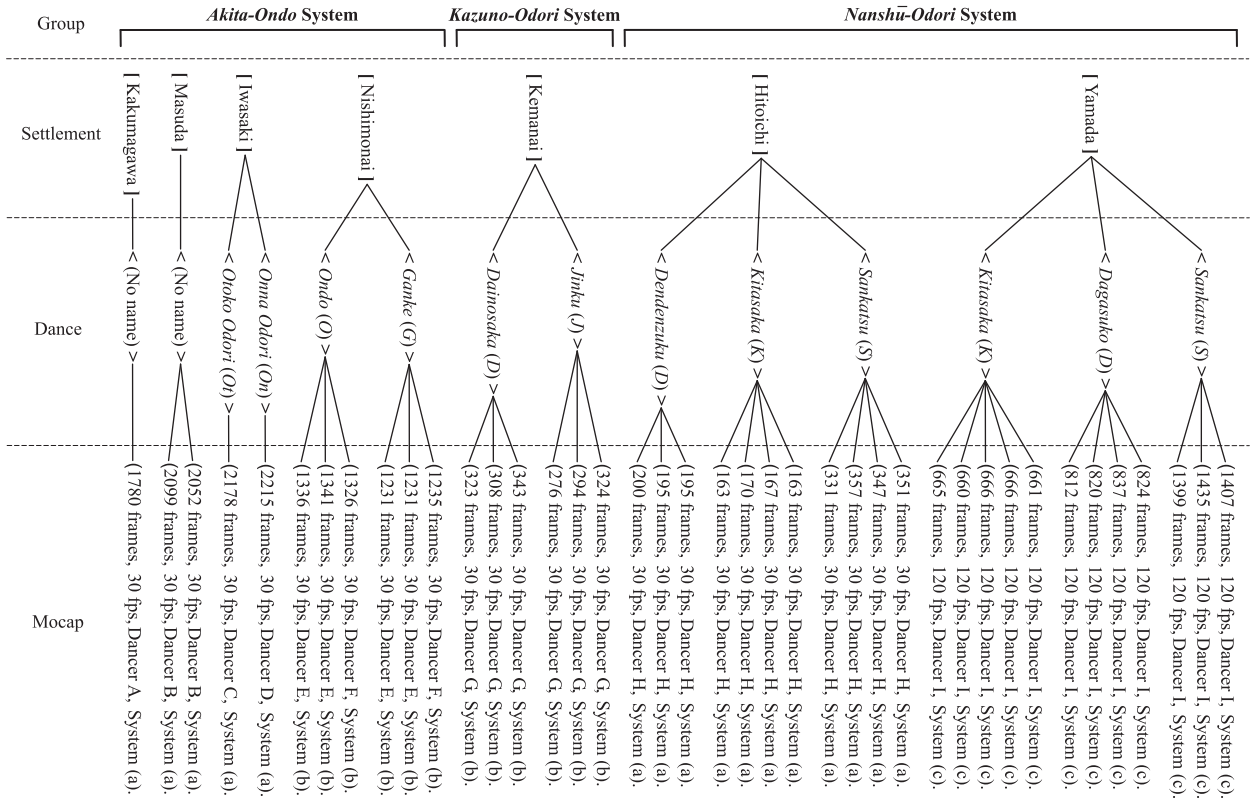

The above data were acquired by the authors through the motion-capture experiments in which experienced dancers danced.

System (a): MotionStar Wireless (Ascension Technology Corporation)
(b): MotionStar Wireless with LIBERTY (Polhemus, 2 sets)
(c): MVN (Xsens)

Fig. 6 Hierarchical-structure model of the *Bon Odori* dances of the Akita Prefecture.

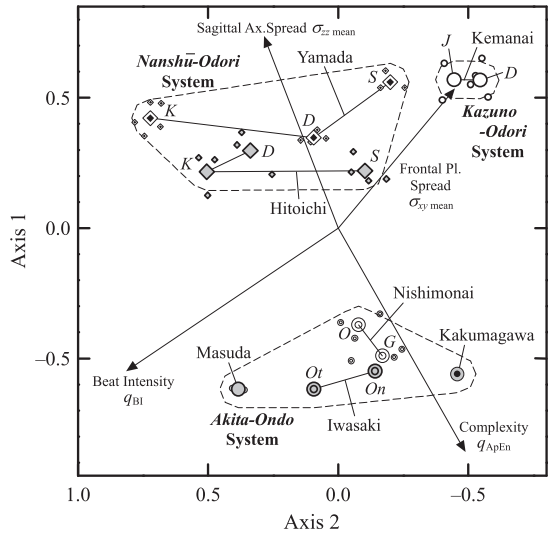

Fig. 7 Motion-characteristic distribution of the *Bon Odori* dances of the Akita Prefecture (obtained by the proposed method).

tem was located at a distance from both the *Kazuno-Odori* and *Nanshū-Odori* Systems, mainly due to the difference in the feature quantity, q_{ApEn}, which represents the "Complexity" of the rhythmic style. From the numbers of frames and the fps values of the corresponding Mocap data streams shown in Fig. 6, one can recognize that the dances of the *Akita-Ondo* System have a much longer performance length than the other groups. This provides the possibility that these dances may include various types of motion patterns. For example, in the case of the settlement Nishimonai, the number of keyposes used to illustrate the motion sequence of *Ondo* ("*O*" in Fig. 7) is twenty five, and that of *Ganke* ("*G*" in Fig. 7) is twenty nine [30]; whereas, the number of keyposes used to illustrate the motion sequence of the dances belonging to the other groups are in the range of six to twelve [31], [32]. This fact suggests that the dances of the *Akita-Ondo* System have many motion patterns contributing to the complexity of motion sequences. The results obtained from the scatter plot are consistent with this tendency.

It is also seen that the axis of the feature quantity, $\sigma_{zz\,\mathrm{mean}}$, representing "Sagittal Ax. Spread," is nearly in parallel and opposite to that of "Complexity." There are few reports that focus on the variation of sagittal-direction motion with respect to the *Bon Odori* dances of the Akita Prefecture; therefore, new knowledge on the dance may have been obtained by the proposed method. By concurrently considering the above characteristics with the geographic distribution shown in Fig. 2 (a), one can visually recognize that the *Bon Odori* dances of the southern part of the Akita Prefecture are distinguished by their rhythm complexity, whereas those of the northern part are distinguished by the spread of the body segments along the sagittal axis. In the illustration of the motion sequence of the Hitoichi settlement [31], a relatively large number of front-rear-direction movements of the legs exist. As for the case of the Kemanai settlement, the action of reaching out ones arms in a forward direction is seen [32]. These results suggest that the proposed method actually provides clues to un-

© 2018 Information Processing Society of Japan

Table 1 Multiple correlation coefficients between the feature quantities and the coordinates of the scatter plot.

Feature quantity		Correlation coefficient
Time domain		
Beat Intensity	q_{BI}	0.983
Complexity	q_{ApEn}	0.988
Spatial domain		
Frontal Ax. Spread	$\sigma_{xx\,\mathrm{mean}}$	0.342
Vertical Ax. Spread	$\sigma_{yy\,\mathrm{mean}}$	0.298
Sagittal Ax. Spread	$\sigma_{zz\,\mathrm{mean}}$	0.791
Frontal Pl. Spread	$\sigma_{xy\,\mathrm{mean}}$	0.699
Sagittal Pl. Spread	$\sigma_{yz\,\mathrm{mean}}$	0.552
Horizontal Pl. Spread	$\sigma_{zx\,\mathrm{mean}}$	0.355
Frontal Ax. Flctn.	$\sigma_{xx\,\mathrm{SD}}$	0.210
Vertical Ax. Flctn.	$\sigma_{yy\,\mathrm{SD}}$	0.587
Sagittal Ax. Flctn.	$\sigma_{zz\,\mathrm{SD}}$	0.560
Frontal Pl. Flctn.	$\sigma_{xy\,\mathrm{SD}}$	0.564
Sagittal Pl. Flctn.	$\sigma_{yz\,\mathrm{SD}}$	0.652
Horizontal Pl. Flctn.	$\sigma_{zx\,\mathrm{SD}}$	0.142

derstanding the relevance of the motion-characteristic distribution to another property, such as the geographic distribution of the dances.

The dances passed down in the Hitoich settlement are distributed along the axis of the feature quantity, q_{BI}, representing "Beat Intensity." In addition, the dances of the Kemanai settlement were located in the area where "Beat Intensity" is mild. In the case of Hitoichi, the dances *Dendenzuku* ("*D*" in Fig. 7) and *Kitasaka* ("*K*" in Fig. 7) are known to have a quick and dynamic tempo, whereas *Sankatsu* ("*S*" in Fig. 7) has a slow and graceful tempo [31]. With regard to the dances of Kemanai, their choreography is often characterized by elegance and refinement [32], and it was pointed out that this impression was caused by their long between-keypose intervals, i.e., their slow tempo [18]. The obtained results agree with the above characteristics.

It is also seen in Fig. 7 that the dances of Kemanai were characterized by the feature quantity, $\sigma_{xy\,\mathrm{mean}}$, which represents "Frontal Pl. Spread." In fact, the action of reaching out the arms in a transverse direction is known as a distinctive motion in these dances [18], and this action causes the spread of the body segments on the frontal plane. This characteristic was reflected in the obtained scatter plot. As a whole, the motion-characteristic distribution of the *Bon Odori* dances of the Akita Prefecture was visualized almost exactly, while remaining consistent with the knowledge acquired in previous studies.

Table 1 shows the values of multiple correlation coefficients between the feature quantities and the coordinates of the scatter plot (calculated by using Eqs. (18) to (21)). It is noted that the feature quantities of the time-domain motion characteristics (i.e., q_{BI} and q_{ApEn}) gave large values compared with those of the spatial-domain motion characteristics. This suggests that the condition of temporal motion-speed variation had a significant influence on the motion-characteristic distribution of the *Bon Odori* dances of Akita Prefecture. This property could have been extracted by separately analyzing the time-domain and spatial-domain motion characteristics.

4.3 Discussion

To discuss the effectiveness of the proposed method, we compare the results shown in "4.2 Results" with those obtained by another analysis method. We use a technique called principal component analysis (PCA) [25], which is known as a typical dimensionality-reduction method. In the analysis, PCA is applied to a set of the fourteen-dimensional feature vectors extracted from all the Mocap data streams shown in Fig. 6, and the location of each dance is determined by calculating the centroid of the Mocap data streams belonging to it.

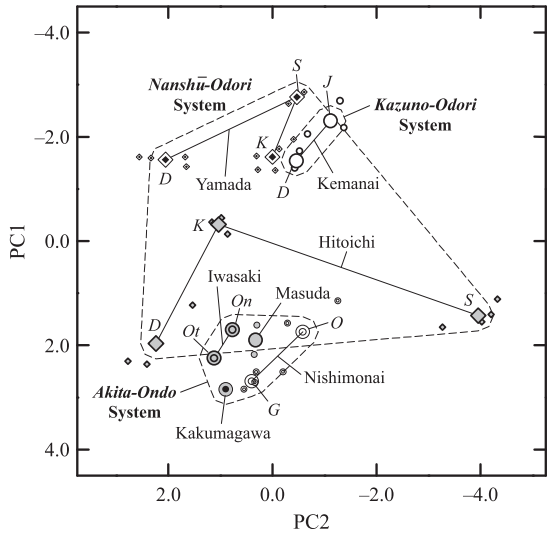

Fig. 8 Motion-characteristic distribution of the *Bon Odori* dances of the Akita Prefecture (obtained by PCA).

Table 2 Components of the eigenvectors obtained by PCA.

Feature quantity		PC1	PC2
Time domain			
Beat Intensity	q_{BI}	0.032	0.182
Complexity	q_{ApEn}	0.382	0.037
Spatial domain			
Frontal Ax. Spread	$\sigma_{xx\,\mathrm{mean}}$	−0.086	0.303
Vertical Ax. Spread	$\sigma_{yy\,\mathrm{mean}}$	0.048	0.461
Sagittal Ax. Spread	$\sigma_{zz\,\mathrm{mean}}$	−0.422	−0.050
Frontal Pl. Spread	$\sigma_{xy\,\mathrm{mean}}$	−0.378	−0.173
Sagittal Pl. Spread	$\sigma_{yz\,\mathrm{mean}}$	−0.308	0.296
Horizontal Pl. Spread	$\sigma_{zx\,\mathrm{mean}}$	−0.180	−0.479
Frontal Ax. Flctn.	$\sigma_{xx\,\mathrm{SD}}$	−0.186	0.194
Vertical Ax. Flctn.	$\sigma_{yy\,\mathrm{SD}}$	0.257	0.229
Sagittal Ax. Flctn.	$\sigma_{zz\,\mathrm{SD}}$	−0.426	0.143
Frontal Pl. Flctn.	$\sigma_{xy\,\mathrm{SD}}$	−0.007	0.149
Sagittal Pl. Flctn.	$\sigma_{yz\,\mathrm{SD}}$	−0.096	0.418
Horizontal Pl. Flctn.	$\sigma_{zx\,\mathrm{SD}}$	−0.323	0.056
Contribution rate		26.0%	19.9%

Figure 8 and **Table 2** show the scatter plot and the component values of the eigenvectors obtained by PCA. The items and scales of the axes of the scatter plot were adjusted in the same manner as the case presented in Fig. 7. In Table 2, the eigenvector of PC1 (corresponding to the vertical axis of Fig. 8) gives high component values to the following feature quantities: q_{ApEn} ("Complexity"), $\sigma_{zz\,\mathrm{mean}}$ ("Sagittal Ax. Spread"), and $\sigma_{zz\,\mathrm{SD}}$ ("Sagittal Ax. Flctn."). The eigenvector of of PC2 (corresponding to the horizontal axis of Fig. 8) gives high component values to $\sigma_{yy\,\mathrm{mean}}$ ("Vertical Ax. Spread"), $\sigma_{zx\,\mathrm{mean}}$ ("Horizontal Pl. Spread"), and $\sigma_{yz\,\mathrm{SD}}$ ("Sagittal Pl. Flctn."). This means that the vertical axis almost corresponds to the combination of the axes of "Complexity" and "Sagittal Ax. Spread" in Fig. 7, whereas there is no axis corresponding to the horizontal axis of Fig. 8.

It is seen in Fig. 8 that the three groups were not clearly sepa-

© 2018 Information Processing Society of Japan

rated from one another. In the case of Fig. 7, in which the groups were clearly separated, the feature quantities "Complexity" and "Beat Intensity" played important roles as already shown in the correlation-coefficient values of Table 1. These time-domain feature quantities, occupying only two of the fourteen components of the feature vector, may have been underestimated in PCA. In fact, the component values of the eigenvectors corresponding to the feature quantity, q_{BI}, representing "Beat Intensity," are extremely small in both PC1 and PC2, as shown in Table 2.

However, in Fig. 8, the dances of the Kakumagawa and Iwasaki settlments were located at positions close to one another. In Fig. 7, the Kakumagawa and Iwasaki dances were located at positions far from each other. As shown in Fig. 6, only a single Mocap data stream is provided for each of the Kakumagawa and Iwasaki dances. In PCA, the same weight is assigned not to each *set* of the Mocap data streams belonging to the same dance, but to each *single* Mocap data stream. This may have caused the underestimation of the dances of Kakumagawa and Iwasaki. This suggests that the results of PCA show the effectiveness of the proposed method on some level.

As shown in the above results, the motion-characteristic distribution of the folk dances passed down in certain areas is systematically and quantitatively visualized by the proposed method. In the visualization process, fourteen feature quantities are used. As mentioned in the last paragraph of "2. Related Work," these quantities represent only the overall tendency of the motion style of each Mocap data stream. This means that the information on *motion content* [*5], which includes that of the structure of a motion sequence along the time axis, cannot be sufficiently extracted by the proposed method. Additional work is needed to address this issue.

5. Conclusion

The main contribution of this study is to provide a technique to systematically visualize the motion-characteristic distribution of Japanese folk dances passed down in a certain area. We adopted an approach that utilizes Mocap data to make it possible to understand the distribution based on objective quantitative analysis. The visualization process was systematized by separating it into the three stages, i.e., the modeling of the relationship among Mocap data, folk dances, and settlements, the extraction of motion characteristics from Mocap data streams, and the visualization of the distribution in a two-dimensional scatter plot. The analysis results demonstrated the effectiveness of the proposed method to a certain extent. However, the example application is still limited to the dances of only one area. In addition, the proposed method does not use a restricted condition in Japanese folk dance, and there still remains a possibility of visualizing another dance category. Therefore, future work will be required to clarify the application range of the proposed method.

Acknowledgments This study was supported by Grants-in-Aid for Scientific Research (No.JP26370942) of Japan Society for the Promotion of Science. The motion-capture data of the *Bon Odori* dances passed down in the settlement Yamada were provided by Akita University's Center of Community Project "Regional Development Aimed at Promoting an Independent Aging Society in Which All Individuals Have Value." We deeply regret the death of Mr. Takaaki Kaiga, one of the authors of this paper, who passed away after a struggle with his disease on the 1st May, 2017.

[*5] According to Ref. [33], the "motion content" consists of a structure of the sequence of actions in a given human motion, including the information on the spatial as well as time domain, such as "a kick of the right foot followed by a punch."

References

[1] Thornbury, B.E.: *The Folk Performing Arts*, State University of New York Press (1997).
[2] Lancashire, T.A.: *An Introduction to Japanese Folk Performing Arts*, Ashgate (2011).
[3] Mimuro, K.: An Introduction to a Study on the Traditional Folk Dance of Japan – With Special Reference to Traditional Folk Dances in the Kibi District, *Bulletin of School of Education, Okayama University*, Vol.18, pp.154–173 (1964) (in Japanese).
[4] Kitagawa, M. and Windsor, B.: *MoCap for Artists*, Focal Press (2008).
[5] Miura, T., Kaiga, T., Matsumoto, N., Katsura, H., Shibata, T., Tajima, K. and Tamamoto, H.: Characterization of Motion Capture Data by Motion Speed Variation, *IEEJ Trans. Electronics, Information and Systems*, Vol.133, No.4, pp.906–907 (2013).
[6] Miura, T., Matsumoto, N., Kaiga, T., Katsura, H., Tajima, K. and Tamamoto, H.: Indexing of Motion Capture Data Using Feature Vectors Derived from Posture Variation, *J. Inf. Process.*, Vol.21, No.2, pp.358–361 (2013).
[7] Averbuch, I.: Shamanic Dance in Japan – The Choreography of Possession in Kagura Performance, *Asian Folklore Studies*, Vol.57, pp.293–329 (1998).
[8] Mimuro, K.: A Study of the Shiraishi Odori (Folk Dance) in the Shiraishi Island – With Special Reference to Its Eurythmic and Musical Expressions, *Bulletin of School of Education, Okayama University*, Vol.19, pp.31–49 (1965) (in Japanese).
[9] Mimuro, K.: A Rhythmic Study of Bon Odori in Okayama Prefecture – Its Geographical Distribution, *Bulletin of School of Education, Okayama University*, Vol.49, pp.77–102 (1978) (in Japanese).
[10] Yamada, A.: Hand Gestures and Steps of the Bon-Dance, *Bulletin of the Faculty of Education, Kochi University*, Vol.69, pp.203–218 (2009) (in Japanese).
[11] Usui, Y., Sato, K. and Watabe, S.: The Effect of Motion Capture on Learning Japanese Traditional Folk Dance, Herrington, J., Couros, A. and Irvine, V. (Eds.): *Proc. EdMedia: World Conference on Educational Media and Technology 2013*, pp.2320–2325 (2013).
[12] Kitsikidis, A., Boulgouris, N.V., Dimitropoulos, K. and Grammalidis, N.: Unsupervised Dance Motion Patterns Classification from Fused Skeletal Data using Exemplar-based HMMs, *International Journal of Heritage in the Digital Era*, Vol.4, No.2, pp.209–220 (2015).
[13] Boulgouris, N.V. and Huang, X.: Gait Recognition Using HMMs and Dual Discriminative Observations for Sub-dynamics Analysis, *IEEE Trans. Image Processing*, Vol.22, No.9, pp.3636–3647 (2013).
[14] Aristidou, A., Stavrakis, E. and Chrysanthou, Y.: Motion Analysis for Folk Dance Evaluation, *Proc. EUROGRAPHICS Workshop on Graphics and Cultural Heritage*, pp.55–64 (2014).
[15] Bartenieff, I. and Lewis, D.: *Body Movement: Coping with the Environment*, Gordon and Breach Science Publishers (1980).
[16] Japan Broadcasting Corporation (Ed.): *Tōhoku Min'yōshu Akita Ken* (*A Collection of Folk Songs of Tohoku Region: Akita Prefecture*), Japan Broadcast Publishing Association (1957) (in Japanese).
[17] Mimura, Y.: *Hiroshima no Kagura Tanbō* (*An inquire into Kagura of Hiroshima*), Nannansha (2004) (in Japanese).
[18] Miura, T., Kaiga, T., Katsura, H., Shibata, T., Tajima, K. and Tamamoto, H.: Quantitative Motion Analysis of the Japanese Folk Dance "Hitoichi Bon Odori," *IPSJ Symposium Series*, Vol.2013, No.4, pp.167–174 (2013).
[19] Pincus, S.M.: Approximate Entropy as a Measure of System Complexity, *Proc. Natl. Acad. Sci. USA*, Vol.88, pp.2297–2301 (1991).
[20] Kaffashi, F., Foglyano, R., Wilson, C.G. and Loparo, K.A.: The Effect of Time Delay on Approximate & Sample Entropy Calculations, *Physica D*, Vol.237, No.23, pp.3069–3074 (2008).
[21] Manis, G.: Fast Computation of Approximate Entropy, *Computer Methods and Programs in Biomedicine*, Vol.91, No.1, pp.48–54 (2008).
[22] Bartlett, R.: *Introduction to Sports Biomechanics*, 2nd ed., Routledge (2007).
[23] Miura, T., Kaiga, T., Shibata, T., Katsura, H., Uemura, M., Tajima,

© 2018 Information Processing Society of Japan

K. and Tamamoto, H.: Motion Characteristics of Bon Odori Dances in Areas along Ushu Kaido Road in Akita Domain, *IPSJ Symposium Series*, Vol.2015, No.2, pp.269–276 (2015).
[24] Rubner, Y., Tomasi, C. and Guibas, L.J.: The Earth Mover's Distance as a Metric for Image Retrieval, *International Journal of Computer Vision*, Vol.40, No.2, pp.99–121 (2000).
[25] Hair, Jr., J.F., Black, W.C., Babin, B.J. and Anderson, R.E.: *Multivariate Data Analysis*, 7th ed., Pearson Education Inc. (2010).
[26] Tasker, G.D.: Hydrologic Regression with Weighted Least Squares, *Water Resources Research*, Vol.16, No.6, pp.1107–1113 (1980).
[27] Skiena, S.S.: *The Algorithm Design Manual*, 2nd ed., Springer (2008).
[28] Bland, J.M, and Altman, D.G.: Calculating Correlation Coefficients with Repeated Observations: Part 2 – Correlation between Subjects, *BMJ*, Vol.310, p.633 (1995).
[29] Miura, T., Kaiga, T., Shibata, T., Katsura, H., Tajima, K. and Tamamoto, H.: Utilization of Motion Capture Data for Research on Folk Performing Arts of Akita Prefecture, *IPSJ SIG Technical Report*, Vol.2015-CH-108, No.5, pp.1–6 (2015) (in Japanese).
[30] Kosaka, T.: *Nishimonai Bon Odori – Waga Kokoro no Genfūkei* (*Nishimonai Bon Odori – The Landscape of My Heart*), Kageshobō (2002) (in Japanese).
[31] Akita-Ken Hachirōgata-Machi Kyōiku Iinkai (Education Board of Hachirogata Town, Akita Prefecture), ed.: *Hitoichi Bon Odori Chōsa Hōkokusho* (*The Search Report on Hitoichi Bon Odori*), Akita-Ken Hachirōgata-Machi Kyōiku Iinkai (2005) (in Japanese).
[32] Yanagisawa, T.: *Kemanai no Bon Odori* (*Bon Odori of Kemanai*), privately published (1999) (in Japanese).
[33] Müller, M., Röder, T. and Clausen, M.: Efficient Content-Based Retrieval of Motion Capture Data, *ACM Trans. Graphics* (*Proc. ACM SIGGRAPH 2005*), Vol.24, No.3, pp.677–685 (2005).

Takeshi Miura received his D.Eng. degree in electrical engineering from Hokkaido University in 1998. He is currently an associate professor in the Department of Electrical-Electronic-Computer Engineering, Graduate School of Engineering Science, Akita University.

Takaaki Kaiga received his M.E. degree in mechanical engineering from Ibaraki University in 1995. Since 1996, he had been with the computer division of Digital Art Factory, Warabi-za Co., Ltd. He died after a struggle with his disease in May, 2017.

Takeshi Shibata received his D.Eng. degree in electronic and computer system engineering from Akita University in 2012. He is currently an assistant professor in the College of Information and Systems, Muroran Institute of Technology. His research interests include virtual reality technique and archiving and handing-down technique for traditional folk dances.

Madoka Uemura received her Ph.D. from the University of Tokyo in 2013. She is currently an associate professor in the Faculty of Education and Human Studies, Akita University.

Katsubumi Tajima received his D.Eng. degree in electrical engineering from Tohoku University in 1998. He is a professor in the Cooperative Major in Life Cycle Design Engineering, Graduate School of Engineering Science, Akita University.

Hideo Tamamoto received his D.Eng. degree in electrical engineering from the University of Tokyo in 1976. He is currently a researcher at Tohoku University of Community Service and Science. His research interests include design-for-testability of logic circuits, archiving and handing-down technique for traditional folk dances.

© 2018 Information Processing Society of Japan